The Journal of Chemical Physics

Percolation probability in a system of cylindrical particles

Cite as: J. Chem. Phys. **149**, 144904 (2018); https://doi.org/10.1063/1.5041326
Submitted: 24 May 2018 . Accepted: 25 September 2018 . Published Online: 12 October 2018

Anatoly Golovnev, and Matthew E. Suss

AIP Publishing

Percolation probability in a system of cylindrical particles

Anatoly Golovnev[a] and Matthew E. Suss[a]
Faculty of Mechanical Engineering, Technion—Israel Institute of Technology, Haifa, Israel

(Received 24 May 2018; accepted 25 September 2018; published online 12 October 2018)

A broad variety of materials, ranging from composites and heat transfer nano-fluids to electrochemical energy storage electrodes, widely employ cylindrical particles of various aspect ratios, such as carbon nanotubes. These particles are generally excellent conductors of heat and electricity and when dispersed in a continuous medium influence dramatically the transport properties of the heterogeneous material by forming a percolating network. Numerous theories exist to predict key parameters such as particle concentration at the percolation threshold and transport properties at concentrations beyond the threshold. The microstructure formed by connecting particles in the material is an important determinant toward such parameters but often requires complex numerical models to resolve. In this paper, we present an analytical, probabilistic model capturing the microstructure of a system of randomly positioned, soft-core, cylindrical particles with a finite aspect ratio, valid at arbitrary particle concentration. Our analytical framework allows for the calculation of the particle contact number distribution and percolation probability of the particle system. We show that our analytical model is more accurate than excluded volume theory for predicting the percolation threshold for spherocylinders of finite aspect ratios, and agrees well with the corresponding numerical results. Our theory describes the percolating network topology above the percolation threshold and can serve as the foundation for analytical composition-structure-property relationships for heterogeneous materials with conducting cylindrical particles. *Published by AIP Publishing.* https://doi.org/10.1063/1.5041326

I. INTRODUCTION

Numerous engineered materials involve the addition of a particulate electrically conductive solid phase to an insulating solid or fluid supporting phase. This addition can greatly improve the electric or heat conductivity compared to the continuous phase alone, often by many orders of magnitude.[1,2] At a certain particle concentration known as the percolation threshold, an interconnected particle network spans the material. This is sometimes referred to more specifically as geometric percolation, as it does not necessarily coincide with electron transport spanning the discontinuous particle phase. The presence of thin layers of the insulating supporting phase at the point of contact between conductive particles can inhibit electric percolation, even at concentrations beyond that of geometric percolation. Thus, the resulting transport properties of the heterogeneous material are determined by both the microstructure of the percolating network and also the particulars of the transport mechanism between individual particles in this network (e.g., electron tunneling).[3,4]

One prominent example of such materials is nanocomposites,[5–7] in which nanoscale conductive filler particles are mixed together with a polymer, and the mixture is solidified into the composite. Nanocomposites are used as structural elements with the filler network serving as an in-built electromagnetic interference shield, such as in aircraft.[8] Another example is the emerging use of flowable electrodes in electrochemical systems which store energy or desalinate water.[9–12] In such systems, conductive particles are suspended in an electrically insulating yet ionically conductive electrolyte, and the entire suspension is pumped through a charging or discharging cell. Electrons transport through the percolating network formed by the solid particles, in order to capacitively charge the solid particles or allow for local electrochemical reactions at solid-liquid interfaces. While such flowable electrodes are dynamic at the micro(particle) level, they nonetheless can deliver time-invariant transport properties on the system level. Thus, the network structure-material function relationships underpinning static nanocomposites may also form a useful basis for describing flowable electrodes.

Once such a heterogeneous material attains electric percolation, the addition of conductive particles generally increases the network's interconnectivity, which improves the materials overall conductivity. However, in practice, there is an upper limit to particle concentration. In the case of nanocomposites, it is desirable to maintain the structural characteristics of the polymer, and thus particle concentration must be kept low, often less than 1 vol. %.[5] For a flowable electrode, the suspension viscosity increases with increasing particle loading, and above roughly 10 vol. %, the suspension behaves as a gel and is no longer able to be pumped effectively.[13] Thus, conductive particles with high aspect ratios, such as carbon nanotubes (CNTs), are widely used for these applications as they generally possess very

[a]Authors to whom correspondence should be addressed: Anatoly.Golovnev@gmail.com and mesuss@me.technion.ac.il

low percolation thresholds while enabling among the highest measured material conductivities to date.[2,14] In order to maximize performance within often-strict particle loading constraints, it is crucial to develop accurate and simple relationships between the particle aspect ratio and loading to the percolation threshold and percolating network conductivity.[15]

Despite the importance of microstructures toward determining bulk properties of the heterogeneous material, most theories do not explicitly consider microstructures or alternatively use complex numerical models to resolve the microstructure. For example, the widely used excluded volume theory[16–18] assigns to each particle a volume within which the centres of other particles cannot enter, called the excluded volume. When a particle intrudes the excluded volume of another particle, it is assumed that the two particles come in contact. At a certain particle concentration, the particles' excluded volumes fill up all space and begin to overlap, which is considered to be the onset of percolation. The latter provides a simple analytical prediction of the percolation threshold but does not explicitly account for the microstructure formed by the conductive particles. As a result, excluded volume theory generally underestimates the measured value for the percolation threshold, although gaining accuracy as the particle aspect ratio rises.[18] Alternatively, the connectedness percolation theory[16,19,20] makes use of the Ornstein-Zernike equation which was originally applied to describe the molecular structure of liquids. This theory expresses the average particle cluster size via the so-called pair connectedness function which describes the probability that two particles at a certain distance from each other belong to the same cluster. When the average cluster size diverges, percolation begins. The connectedness percolation theory and the excluded volume theory agree that the percolation threshold concentration is inversely proportional to the particle aspect ratio but disagree on the influence of dispersity of particle lengths on the percolation threshold.[19] Also, both the excluded volume and connectedness percolation theories predict only a percolation threshold and do not predict network topology or material properties at particle concentrations of interest above the threshold.

Toward predicting electric conductivity of percolating heterogenous materials, one widely used model invokes the scaling hypothesis, which states that at the vicinity of the percolation threshold, the conductivity scales as the power law,[21,22] $\sigma = \sigma_0(\psi - \psi_p)^t$. Here σ is the heterogeneous material conductivity, σ_0 is a prefactor, ψ is the volume loading of conductive particles, ψ_p is the loading at the percolation threshold, and t is the exponent. The exponent is predicted to be between 1.2 and 2, with a smaller exponent predicted for increased aspect ratios.[23,25] By contrast, experiments have yielded varying and significantly higher exponents of best fit,[5] up to 10, which is generally attributed to the effect of interparticle resistances rendering a portion of the geometrically percolating network effectively unable to accept electric charge.[1] Apart from the scaling hypothesis, various effective medium approximations have been adopted.[23,27,28] Such models employ the formalism of graph theory and usually are very advanced mathematically. They make various predictions depending on the approximation chosen. Another cause of uncertainty comes from modeling a resistance of contacts between particles, which is essential only for finding electric conductivity and believed to be due to electron tunneling.[29] However, the main disadvantage of the models reviewed above is that they account only implicitly, or sometimes even completely neglect, the suspension microstructure which is responsible for composite material bulk properties.[26,32]

We here develop an analytical probabilistic model which captures explicitly the microstructure of suspensions of high aspect ratio rods, valid over a wide range of particle concentrations: below and above the percolation threshold. In Sec. II, we derive the distribution of contacts between particles. In Sec. III, we discuss the particle cluster size distribution, including the infinite cluster which is the percolation network. We find how many particles the network consists of and how interconnected, or how "dense," the network is. Via accounting for network microstructures analytically, we can predict the percolation threshold with significantly more accuracy than excluded volume theory and reproduce the predicted percolation threshold attained via numerical models. In the future, the analytical model presented here can be used as a foundation to predict various macroscopic properties of heterogeneous materials employing high aspect ratio conductive particles, such as electric conductivity or suspension viscosity.

II. PARTICLE CONTACT NUMBER DISTRIBUTION

Let us consider a system of independent, non-interacting, identical, cylindrical particles with diameter d and length l suspended in an inert medium. The particles are randomly positioned and randomly oriented. The aim of this section is to find the contact number distribution, $P_\psi(k)$, which is the fraction of particles having contacts with k other particles at a given particle volume fraction, ψ, defined as the volume of all particles divided by the total volume of the heterogeneous system. Following from the definition, $\sum_{k=0}^{\infty} P_\psi(k) = 1$ at any ψ. We assume that the system dimension is several orders of magnitude larger than the particle dimension. Therefore, even for dynamic networks where particles are in motion, we expect that fluctuations of $P_\psi(k)$ in time are negligible and $P_\psi(k)$ can be considered as time independent. At a snapshot, $P_\psi(k)$ can also be interpreted as the probability that a randomly chosen particle has k contacts in both dynamic and static networks. Throughout the paper, we will use both the definitions for $P_\psi(k)$ interchangeably. In terms of the theory of random graphs, $P_\psi(k)$ is called a degree distribution and k is called a degree of a node, where a node denotes a particle.[30]

Let us pick randomly one particle and call it the target particle. To position other particles, we place the end of each particle at a randomly chosen point in space, called the pinpoint, and then rotate the particle by a random angle; see Fig. 1. Because the angle is chosen randomly, it is irrelevant which particle end is taken as the pinpoint. For hard-core particles, not every angle is accessible since particles cannot overlap. In the present paper, we assume that particles are penetrable (called soft-core or ideal particles). Thus here, if the placed

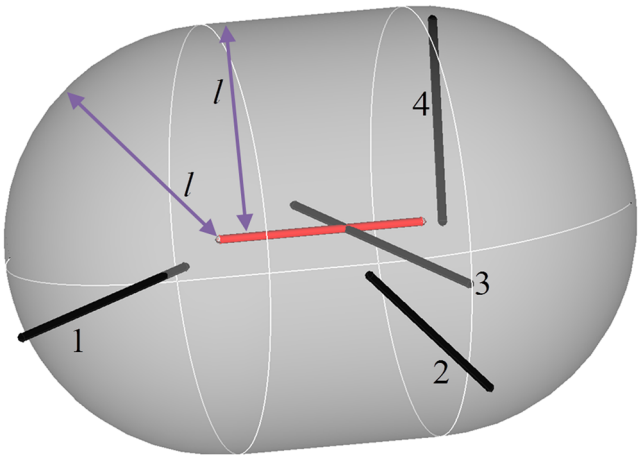

FIG. 1. Schematic of the access volume (shaded gray) consisting of a target particle (in red) and selected placed particles (in black) with an aspect ratio of $l/d = 50$. Particle 3 is in contact with the target particle, while particles 1, 2, and 4 are not in contact.

particle intersects the target particle, we define it as a particle contact. It was demonstrated by simulations[31] that the percolation threshold concentration for soft-core and hard-core rods is noticeably different. In the present work, we are laying the foundation of a new approach and therefore consider only ideal particles as the simplest and most straightforward case.

Let us count how many contacts the target particle has. Because l is finite, only a limited amount of particles can reach the target particle, namely, the particles whose pinpoints are located not farther than l from the target particle. We call the set of such pinpoints the access volume which is a capped cylinder with radius l drawn around the target particle; see Fig. 1. The access volume is given by $V_0 = \pi l^2 \cdot l + \frac{4}{3}\pi l^3 = \frac{7}{3}\pi l^3$ and contains $N + 1$ particles: one target particle and N other particles. We define that a particle lies in the access volume if and only if its pinpoint is in the access volume. By definition, the particle volume fraction is $\psi \equiv \frac{(N+1)V_p}{V_0}$, where V_p is the volume of one particle. Hence,

$$N = \frac{28}{3}\psi\left(\frac{l}{d}\right)^2 - 1. \tag{1}$$

Later in this section, we will show that for relevant ψ the unity term can be neglected. Because N and ψ have a one-to-one relation, we will use $P_N(k)$ and $P_\psi(k)$ interchangeably.

Penetrability of particles makes positioning of one particle independent of positions of other particles. Therefore, instead of placing N particles one-by-one making sure they do not overlap, we can place one particle N times in a row. In the framework of probability theory, each placing is called a Bernoulli trial because it has only two possible outcomes: particles either come in contact or not.[33] Let p be the probability that at one trial the placed particle touches the target particle. Hence, $(1 - p)$ is the probability that the particle misses the target particle. A sequence of independent Bernoulli trials is called a Bernoulli process. In terms of Bernoulli processes, $P_N(k)$ is the probability that out of N trials the target particle is hit exactly k times. Thus,[33] $P_N(k)$ is the binomial distribution,

$$P_N(k) = \frac{N!}{k!(N-k)!}p^k(1-p)^{N-k}. \tag{2}$$

Now we shall find the probability that the placed particle touches the target particle, p. The placed particle can have many different configurations, i.e., orientations and positions. Only some of them correspond to a contact. If these configurations were discrete and equiprobable, then the probability p is defined as a ratio of the number of configurations corresponding to a contact to the number of all possible configurations. Because coordinates and angles are continuous variables, we introduce a configuration space,

$$p \equiv \frac{F}{\Omega}, \tag{3}$$

where F is the volume of configuration space corresponding to a contact and Ω is the total volume of configuration space,

$$\Omega = \iiint \iint dx\,dy\,dz\,\sin(\theta)d\theta\,d\varphi, \tag{4}$$

where the Cartesian coordinates (x, y, z) set the particle pinpoint position, the spherical coordinate angles (θ, φ) set the particle orientation, and the integral is taken over all possible values of $(x, y, z, \theta, \varphi)$. The multiplier $\sin(\theta)$ originates from the spherical coordinate Jacobian. It assures that the probability of the placed particle being directed within a certain solid angle is proportional to the solid angle opening and independent of its orientation. The integral over the position coordinates is the volume of the access volume, $\int\int\int dxdydz = V_0$. Because θ changes from 0 to π, and φ runs from 0 to 2π, $\int\int \sin(\theta)d\theta d\varphi = 4\pi$. Hence,

$$\Omega = \frac{28}{3}\pi^2 l^3. \tag{5}$$

To find F, we need to take the same integral from Eq. (4) but this time only over the configurations $(x, y, z, \theta, \varphi)$ that lead to a particle contact. Obviously, not every configuration qualifies because, for example, two particles can be skew. This rather technical procedure, which requires simple but extensive geometrical construction, can be found in the supplementary material. Here we proceed already with the final result,

$$F = 4\left(\pi - \frac{7}{6}\right)\pi d\,l^2. \tag{6}$$

Note that F contains the excluded volume, V_{ex}; see Refs. 17 and 18 for V_{ex}. Indeed, to draw the excluded volume, the tip of the placed particle should slide on the target particle. All such configurations of the placed particle comprise the excluded volume. F consists of all these "tip touch" configurations plus the configurations where the placed particle touches the target particles with its side. Therefore, $F > V_{ex}$ always. ($F = V_{ex}$ for spheres, which is not considered in the present paper.) For thick rods, "side touch" and "tip touch" correspond to different (θ, φ). However, in the thin rod limit, (θ, φ) for side and tip touches become almost the same, making F and V_{ex} the same functional dependence, $V_{ex} \sim d\,l^2$. Still, in this limit "side touches" bring additional configurations due to different (x, y, z) which are not present in "tip touches," making $F > V_{ex}$ because of the larger prefactor.

Using Eqs. (3), (5), and (6), we find the probability of particle contact at one Bernoulli trial,

$$p = \frac{6\pi - 7}{14\pi^2}\left(\frac{d}{l}\right) \approx 0.270\left(\frac{d}{l}\right). \tag{7}$$

If $l/d > 30$, the smallest aspect ratio considered in the present paper, then $p < 0.01$. In this limit, a simpler Poisson distribution can be used,[33] with a good accuracy even at arbitrary low N. Hence, Eq. (2) becomes

$$P_N(k) \approx \frac{(pN)^k}{k!}\exp(-pN). \tag{8}$$

Note that there is only one parameter in Eq. (8), pN. Therefore, our model predicts that this is the only parameter which defines the size and topology of the percolation network or any other cluster. An ideologically similar result is known in graph theory where the emergence of a certain kind of a cluster, called the giant component, is governed by the same parameter.[30] Because this parameter is so important, we will introduce a special letter for it, $\alpha \equiv pN$, and will call it "adjusted concentration." From Eqs. (1) and (7),

$$\alpha \equiv pN = \frac{2}{3}\left(\frac{6\pi - 7}{\pi}\right)\psi\frac{l}{d} \approx 2.515\psi\frac{l}{d}. \tag{9}$$

The mathematical meaning of α is the expected value of $P_N(k)$.[33] Because α is the only variable in Eq. (8), it suggests a scaling relation, in that the system topology is identical for constant adjusted concentration. Such a relation was already derived in the framework of the random contact model and the excluded volume theory,[37] stating that $\psi\frac{l}{d}$ is proportional to the average number of contacts per particle, however, without stating explicitly that topological properties of the system are defined by this parameter. Also, our derivation is more fundamental because it is based only on the assumption of particle random positioning. One specific case of this scaling law is well known, namely, the excluded volume theory states[18] that the percolation threshold occurs when $\psi\frac{l}{d} = 0.5$. Inserting $l/d = 30$ and $\psi\frac{l}{d} = 0.5$ into Eq. (1) gives $N = 140$, meaning that the unity term in Eq. (1) can be neglected.

III. PERCOLATION NETWORK

In Sec. II, we described the environment of a single particle. In the present section, we will deal with particle clusters. Following Sec. II, we know that the target particle has a probability $P_N(k)$ of having k contacts. Let us call these k particles a step zero. The step zero particles touch the target particle and k_1 other particles. These k_1 particles are step one. Each of the step one particles has one or more contacts to the corresponding step zero particles and also may have some other contacts. Only these latter contacts belong to the step two. If we continue our "walk" and find that we can make an infinite number of steps, then the target particle belongs to the percolation network. If at a certain step there are no contacts to a subsequent step, then the target particle belongs to a finite cluster. Note that particles in proceeding steps appear with a probability, meaning that the ability to make each step is not certain. Therefore, if we happen to circle a geometric loop of particles, each proceeding circle will have a smaller probability, and eventually the probability of being able to keep circling the loop will shrink to zero. To be able to keep "walking" infinitely, new particles should keep appearing on our path, which is possible only on an infinite cluster. Because our procedure allows for multiple counting, it is not appropriate toward determining properties of finite clusters, such as a finite cluster size. Our procedure has an analogy to a Bethe lattice,[34,35] except that in a Bethe lattice the number of particles in each step is predetermined and multiple counting is forbidden.

Let $P_{k,n}(w)$ be the probability that in step w there are n particles, given there are k particles in step 0. $P_{k,n}(w)$ are the elements of a matrix $\boldsymbol{\pi}_w$ which fully describes the transition from step 0 to step w. Let us consider $\boldsymbol{\pi}_1$. Since we do not restrict the number of contacts a particle can have (the probabilities of an unrealistically high number of contacts are infinitesimal), $\boldsymbol{\pi}_1$ has an infinite amount of rows and columns which are numbered from 0 to infinity. Furthermore, $P_{0,0}(1) = 1$ and $P_{0,n}(1) = 0$ if $n \neq 0$. Although the number of particles in step zero is directly defined by $P_N(k)$, the number of particles in all proceeding steps, $P_{k,n}(w)$ where $w \geq 1$, obeys a different distribution and should employ conditional probability since each particle must have at least one contact to a previous step particle. Thus, for $k = 1$, the number of particles in step one is given by

$$P_{1,n}(1) = P_N(n+1|\text{has at least one contact}) \tag{10}$$

with the condition imposed on the step zero particle indicated behind the vertical bar. Here the step zero particle has $n + 1$ contacts: n contacts to step one particles and one mandatory contact to the target particle. According to the Kolmogorov definition of conditional probability,[33]

$$P_{1,n}(1) = \frac{P_N(n+1)}{1 - P_N(0)} = \frac{1}{(n+1)!}\frac{\alpha^{n+1}e^{-\alpha}}{(1 - e^{-\alpha})}, \tag{11}$$

where $1 - P_N(0)$ is the probability for a particle to have at least one contact. In the supplementary material, we derive the general expression needed to complete all entries to $\boldsymbol{\pi}_1$,

$$P_{k,n}(1) = \frac{\Sigma_{l=1}^{k}(-1)^{k+l}\binom{k}{l}l^{n+k}}{(n+k)!}\frac{\alpha^{n+k}e^{-k\alpha}}{(1 - e^{-\alpha})^k}. \tag{12}$$

Equation (12) implies that the number of step one particles is determined only by the number of step zero particles. By the construction of our "walk," the just considered transition from step 0 to step 1 is not different from any further transition. Indeed, the amount of step $w + 1$ particles is set by the step w particles for an arbitrary $w \geq 0$, based on the same distribution, Eq. (12). In probability theory, a sequence of such equivalent transitions is called a simple Markov chain, for which $\boldsymbol{\pi}_w = \boldsymbol{\pi}_1^w$.[33] Hence in principal, Eq. (12) is sufficient to find $\boldsymbol{\pi}_w$ completely. One can significantly simplify the calculations needed by recognizing that we only require $P_{k,0}(w)$, as this represents the final step w along a finite particle cluster. In other words, $P_{k,0}(w)$ gives the probability that the target particle does not belong to the percolation network. In the supplementary material, we derive a recurrence relation

$$P_{k,0}(w+1) = \left(\frac{e^{\alpha P_{1,0}(w)} - 1}{P_{1,0}(w)(e^{\alpha} - 1)}\right)^k. \tag{13}$$

The expression in the brackets in Eq. (13) is independent of k and equals $P_{1,0}(w+1)$. Hence, $P_{k,0}(w) = P_{1,0}(w)^k$, which has a simple physical interpretation. Each step zero particle is a potential path to connect to the percolation network which breaks off with the probability $P_{1,0}(w) \le 1$. Hence, k independent paths break off with the probability $P_{1,0}(w)^k \le P_{1,0}(w)$, which mathematically demonstrates that particles with a higher number of contacts, i.e., with higher k, are more probable to belong to the percolation network.

In Fig. 2, $P_{1,0}(w)$ found from Eq. (13) is plotted for various w as a function of particle concentration. One can see that the recurrence relation given by Eq. (13) converges at $w \to \infty$. $P_{1,0}(500)$ coincides with $P_{1,0}(10\,000)$ on the scale of the figure and therefore can be taken as an approximation for $P_{1,0}(\infty)$. Physically, the difference between $P_{1,0}(w_1)$ and $P_{1,0}(w_2)$ is due to the clusters which have more than w_1 but less than w_2 steps. For example, at the adjusted concentration $\alpha = 3$, all finite clusters consist of no more than 5 steps. Around $\alpha = 1.2$, the difference between $P_{1,0}(5)$ and $P_{1,0}(20)$ is significant and roughly 0.08. By contrast, the difference between $P_{1,0}(20)$ and $P_{1,0}(50)$ is negligibly small, indicating a small population of clusters with steps between 20 and 50.

The flat and the decreasing parts of $P_{1,0}(500)$ in Fig. 2 are two branches of the solution to Eq. (13) found at $w \to \infty$. As shown in the supplementary material, $P_{1,0}(\infty)$ cannot be expressed analytically; hence it is not exponential. However, $P_{1,0}(\infty)$, as well as $P_{1,0}(500)$, can be fit excellently above a percolation threshold by a sum of two exponentials,

$$f(\alpha) = 9.24e^{-2.205\alpha} + 2.91e^{-0.873\alpha}. \tag{14}$$

Such a functional form might have been expected intuitively, though not predicted rigorously. Complex disordered systems, such as networks and also glasses, which might resemble networks due to the lack of long-range order,[36] usually exhibit two exponential processes: one fast and one slow. To fit $P_{1,0}(\infty)$ at every α, we will use the Heaviside step function, $H(\alpha)$,

$$P_{1,0}(\infty) = f(\alpha) + [1 - f(\alpha)]H(1.6 - \alpha). \tag{15}$$

In Fig. 2, the sharp elbow of $P_{1,0}(500)$ from unity to less than unity signifies the appearance of an infinite cluster and, thus, defines the percolation threshold at $\alpha \approx 1.6$ (see the supplementary material for the calculation of its position). In Fig. 3, we compare our theoretical prediction for the percolation threshold with the excluded volume theory and with the data taken from Ref. 18 where several numerical and experimental studies were fit by the curve

$$\psi_c^{num} = \frac{\left(1 + 3.2\left(\frac{2l}{d}\right)^{0.46}\right)}{\frac{\pi}{2}\frac{d}{l} + 2\frac{l}{d} + (3+\pi)} \approx 0.5\left(\frac{l}{d}\right)^{-1}\left(1 + 3.2\left(\frac{2l}{d}\right)^{0.46}\right). \tag{16}$$

The denominator in the exact formulation in Eq. (16) is the exact prediction of the excluded volume theory (blue curve in Fig. 3), and the numerator is the result of the fitting (dashed black curve). This curve also fits well the simulations performed in Ref. 31 for ideal rods, depicted in Fig. 3 of Ref. 31. The curve $\psi_c^{ex} = 0.5(l/d)^{-1}$, which corresponds to $\alpha_c^{ex} \approx 1.26$ as per Eq. (9), is the excluded volume theory prediction for a percolation threshold in the high aspect ratio limit (red curve). Figure 3 shows that the percolation threshold predicted by our theory, $\alpha = 1.6$ which is $\psi = 0.63(l/d)^{-1}$, matches excellently the numerical results and holds down to as low as an aspect ratio of 30, giving a reasonably adequate prediction even at $l/d = 10$. This speaks toward the fine capture of the physical phenomenon by our theory, which might come a bit surprising in the close vicinity of the percolation threshold because percolation is a critical phenomenon; hence, collective behavior plays a crucial role.[24] At the critical point, i.e., the percolation threshold, the average cluster size diverges. Close to the critical point, cluster sizes vary from just a few particles to nearly infinite, an effect called critical fluctuations. Microscopic approaches as ours considering single particles might be expected to have difficulty dealing with critical fluctuations. Probably, the difficulties are avoided due to the felicitous method of counting particles. Also, the fit of excluded volume theory to simulation data performed in Ref. 23 suggests that the number of contacts per particle at the percolation threshold

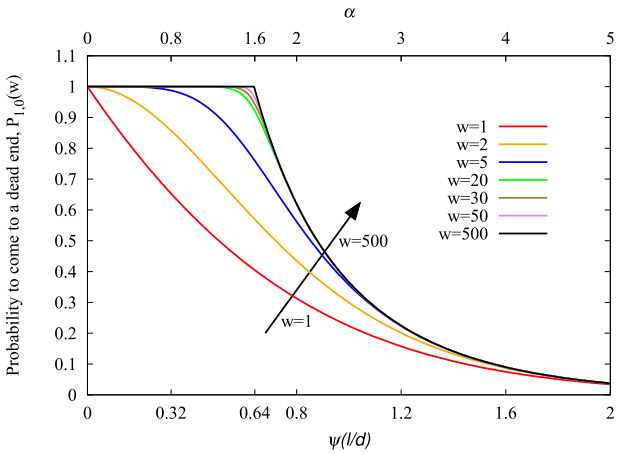

FIG. 2. Probability that the walk along a cluster ends after w steps, $P_{1,0}(w)$, provided that there is only one particle in step zero; see Eq. (13). The upper axis is the adjusted concentration α. The lower axis is the particle volume fraction times particle aspect ratio; see Eq. (9).

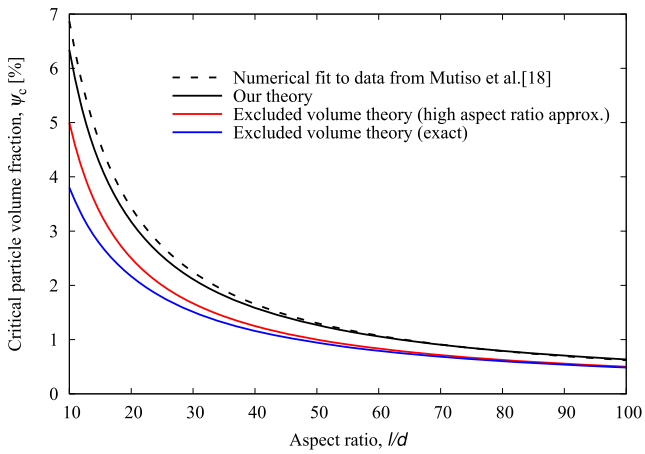

FIG. 3. Predicted particle volume fraction at the percolation threshold as a function of particle aspect ratio. The data fit is taken from Ref. 18. Our theory curve obeys $\psi(l/d) = 0.63$ or equivalently $\alpha = 1.6$. For the other curves, see Eq. (16).

is 1.2, whereas our theory predicts 1.6 since α is the expected value of $P_\psi(k)$. Note in Fig. 3 that excluded volume theory indeed underpredicts the percolation threshold. This is because an overlap of particles' excluded volumes does not guarantee a formation of an infinite cluster.

In order to predict the transport properties of a heterogeneous material, such as a flowable electrode, above a percolation threshold, both the percolation network topology and interparticle resistance to transport are required.[1] We can now utilize our theory toward analytically calculating the network topology. In Sec. II, we define the particle contact number distribution, $P_\psi(k)$, as the probability of a random particle to have k contacts, where ψ is the volume fraction of all particles. Now, let $\widetilde{P_\psi}(k)$ be the contact number distribution for the particles belonging to the percolation network. There are $P_\psi(k)$ particles in step zero of our "walk." They lead to a dead end with the probability $P_{k,0}(\infty) = P_{1,0}(\infty)^k$ as per Eq. (13). If they do not lead to a dead end, then the target particle belongs to the percolation network. Hence,

$$\widetilde{P_\psi}(k) = P_\psi(k) \cdot \left(1 - P_{1,0}(\infty)^k\right). \tag{17}$$

Equation (17) defines the percolation network topology and is thus a crucial result toward an analytical calculation of the heterogeneous material's transport properties. Though $\widetilde{P_\psi}(k)$ is primary, to simplify visualisation, we will plot a percolation probability which is a fraction of particles belonging to the percolation network, $\sum_{k=0}^{\infty} \widetilde{P_\psi}(k)$. Singling out the Poisson distribution from Eq. (17), we get

$$\widetilde{P_\psi}(k) = \frac{\alpha^k e^{-\alpha}}{k!} - \frac{\left[\alpha P_{1,0}(\infty)\right]^k \exp\left[-\alpha P_{1,0}(\infty)\right]}{k!} \times \exp\left[\alpha(P_{1,0}(\infty) - 1)\right], \tag{18}$$

which is trivial to sum up

$$\sum_{k=0}^{\infty} \widetilde{P_\psi}(k) = 1 - \exp\left[\alpha(P_{1,0}(\infty) - 1)\right]. \tag{19}$$

The percolation probability as a function of particle volume fraction is shown in Fig. 4 (black curve). At $\psi(l/d) = 1$, 80% of particles belong to the percolation network and 8% are single; hence, 12% of particles belong to finite size clusters. At $\psi(l/d) = 1.5$, we have 96.5% and 2.3% for network particles and single particles. At $\psi(l/d) = 2$, over 99% of all particles belong to the percolation network.

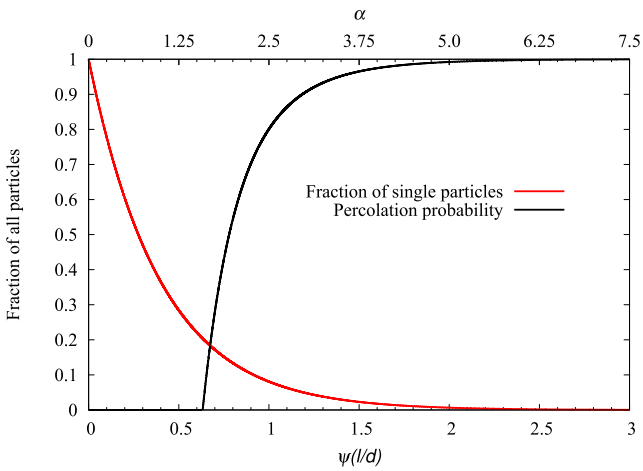

FIG. 4. Predicted percolation probability as a function of particle adjusted concentration α (upper axis) and particle volume fraction times particle aspect ratio (lower axis). The fraction of particles without contacts is shown for comparison.

IV. CONCLUSION

Our goal was to develop an analytical theory describing the structure of a system of randomly oriented penetrable rods and valid for a broad range of their concentrations. The theory should allow further derivation of various bulk properties. In the present paper, we made an analytical prediction of the rod system topology. We found a contact number distribution for a single particle, $P_\psi(k)$, and a contact number distribution for a particle subsystem forming an infinite cluster called a percolation network, $\widetilde{P_\psi}(k)$. Based on $\widetilde{P_\psi}(k)$, we found the fraction of particles in the percolation network, i.e., the percolation probability; see Fig. 4.

We showed that the well-known scaling law $\psi(l/d) = \text{const.}$ is topological in origin and particle systems with the same adjusted concentration, or the same $\psi(l/d)$, are topologically identical. A specific case of this law is the condition for a percolation threshold, namely, $\psi_c(l/d) \approx 0.63$. This condition is in excellent agreement with simulations and comes from an analytical consideration only. At $\psi(l/d) = 2$, nearly every particle belongs to the percolation network. Our theory, without relying on simulations, has a potential for further calculations. For example, one can account for interparticle forces,[38,39] influence of solid interfaces,[14,40] and particle alignment by the electrolyte flow.[41] All these effects lead to an alteration of the probability to touch the target particle, p, in Eq. (7). Future work can also relate bulk material properties to the distributions found in the present paper ($\widetilde{P_\psi}(k)$ to electric conductivity and $P_\psi(k)$ to viscosity).

SUPPLEMENTARY MATERIAL

See supplementary material for some auxiliary calculations mentioned in Secs. II and III, namely, the calculation of a particle contact configuration space volume, and information on evaluating several sums while deriving Eqs. (12) and (13).

ACKNOWLEDGMENTS

This work is supported in part at the Technion by an Aly Kaufman Fellowship. We acknowledge funding from the Israel Science Foundation in the framework of the Israel National Research Center for Electrochemical Propulsion (INREP) project.

[1] R. M. Mutiso and K. I. Winey, Prog. Polym. Sci. **40**, 63–84 (2015).
[2] T. J. Petek, N. C. Hoyt, R. F. Savinell, and J. S. Wainright, J. Electrochem. Soc. **163**(1), A5001–A5009 (2016).
[3] N. Johner, C. Grimaldi, I. Balberg, and P. Ryser, Phys. Rev. B **77**, 174204 (2008).
[4] G. Ambrosetti, N. Johner, C. Grimaldi, T. Maeder, P. Ryser, and A. Danani, J. Appl. Phys. **106**, 016103 (2009).
[5] W. Bauhofer and J. Z. Kovacs, Compos. Sci. Technol. **69**, 1486 (2009).
[6] S. Kale, F. A. Sabet, I. Jasiuk, and M. Ostoja-Starzewski, J. Appl. Phys. **120**, 045105 (2016).

[7]A. V. Kyrylyuk1 and P. van der Schoot, Proc. Natl. Acad. Sci. U. S. A **105**(24), 8221–8226 (2008).
[8]R. Strümpler and J. Glatz-Reichenbach, J. Electroceram. **3**, 329–346 (1999).
[9]T. J. Petek, N. C. Hoyt, R. F. Savinell, and J. S. Wainright, J. Power Sources **294**, 620–626 (2015).
[10]S. Jeon, H. Park, J. Yeo, S. Yang, C. Cho, M. Han, and D. Kim, Energy Environ. Sci. **6**(5), 1471–1475 (2013).
[11]M. Duduta, B. Ho, V. C. Wood, P. Limthongkul, V. E. Brunini, W. C. Carter, and Y. M. Chiang, Adv. Energy Mater. **1**(4), 511–516 (2011).
[12]V. Presser, C. R. Dennison, J. Campos, K. W. Knehr, E. C. Kumbur, and Y. Gogotsi, Adv. Energy Mater. **2**(7), 895–902 (2012).
[13]M. Youssry, L. Madec, P. Soudan, M. Cerbelaud, D. Guyomard, and B. Lestriez, Phys. Chem. Chem. Phys. **15**, 14476 (2013).
[14]H. Parant, G. Muller, T. Le Mercier, J. M. Tarascon, P. Poulin, and A. Colin, Carbon **119**, 10–20 (2017).
[15]A. V. Kyrylyuk1, M. C. Hermant, T. Schilling, B. Klumperman, C. E. Koning, and P. van der Schoot, Nat. Nanotechnol. **6**, 364–369 (2011).
[16]A. L. R. Bug, S. A. Safran, and I. Webman, Phys. Rev. B **33**, 4716–4724 (1986).
[17]I. Balberg, C. H. Anderson, S. Alexander, and N. Wagner, Phys. Rev. B **30**(7), 3933–3943 (1984).
[18]R. M. Mutiso, M. C. Sherrott, J. Li, and K. I. Winey, Phys. Rev. B **86**, 214306 (2012).
[19]R. H. J. Otten and P. van der Schoot, J. Chem. Phys. **134**, 094902 (2011).
[20]R. H. J. Otten and P. van der Schoot, Phys. Rev. Lett. **103**, 225704 (2009).
[21]M. Panda, V. Srinivas, and A. K. Thakur, Results Phys. **5**, 136–141 (2015).
[22]B. I. Halperin, S. Feng, and P. N. Sen, Phys. Rev. Lett. **54**, 2391 (1985).
[23]M. Foygel, R. D. Morris, D. Anez, S. French, and V. L. Sobolev, Phys. Rev. B **71**, 104201 (2005).
[24]J. J. Binney, N. J. Dowrick, A. J. Fisher, and M. E. J. Newman, *The Theory of Critical Phenomena: An Introduction to the Renormalization Group*, 1 ed. (Clarendon Press, 1992).
[25]M. Sahimi, *Applications of Percolation Theory* (Taylor and Francis, London, 1994).
[26]S. Vionnet-Menot, C. Grimaldi, T. Maeder, S. Strassler, and P. Ryser, Phys. Rev. B **71**, 064201 (2005).
[27]L. Gao, X. Zhou, and Y. Ding, Chem. Phys. Lett. **434**, 297–300 (2007).
[28]B. Nigro and C. Grimaldi, Phys. Rev. B **90**, 094202 (2014).
[29]A. Buldum and J. P. Lu, Phys. Rev. B **63**, 161403(R) (2001).
[30]A. L. Barabasi, *Network Science* (Cambridge University Press, 2016).
[31]T. Schilling, M. A. Miller, and P. van der Schoot, Europhys. Lett. **111**(5), 56004 (2015).
[32]S. I. White, R. M. Mutiso, P. M. Vora, D. Jahnke, S. Hsu, J. M. Kikkawa, J. Li, J. E. Fischer, and K. I. Winey, Adv. Funct. Mater. **20**, 2709 (2010).
[33]B. V. Gnedenko, *Theory of Probability* (CRC Press, 1998).
[34]A. P. Chatterjee, J. Chem. Phys. **132**, 224905 (2010).
[35]A. P. Chatterjee, J. Phys.: Condens. Matter **23**, 375101 (2011).
[36]S. Karmakar, J. Phys.: Conf. Ser. **759**, 012008 (2016).
[37]A. P. Philipse, Langmuir **12**, 1127–1133 (1996).
[38]E. J. M. Verwey and J. T. G. Overbeek, *Theory of Stability of Lyophobic Colloids* (Elsevier Amsterdam, 1948).
[39]S. H. Behrens and M. Borkovec, J. Colloid Interface Sci. **225**, 460–465 (2000).
[40]M. Trebbin, D. Steinhauser, J. Perlich, A. Buffet, S. V. Roth, W. Zimmermann, J. Thiele, and S. Frster, Proc. Natl. Acad. Sci. U. S. A. **110**(17), 6706–6711 (2013).
[41]S. I. White, B. A. DiDonna, M. Mu, T. C. Lubensky, and K. I. Winey, Phys. Rev. B **79**, 024301 (2009).